International Journal of Scientific Research in Engineering and Management (IJSREM)
Volume: 09 Issue: 06 | June - 2025 SJIF Rating: 8.586 ISSN: 2582-3930

Comparative Modal Analysis of Engineering Materials for High-Speed Machining Applications Using CATIA

[1]Research Scholar Pawan Sawle, [2]Professor Ghanshyam Dhanera
Department of Mechanical Engineering, BM College of Technology Indore

Abstract- The present research investigates the comparative modal analysis of three different engineering materials - AISI 4140 alloy steel, Ti-6Al-4V titanium alloy, and carbon fiber reinforced polymer (CFRP) - using CATIA software. The study focuses on analyzing and comparing the dynamic characteristics including natural frequencies, modal stress distributions, and displacement patterns for the first ten modes of vibration in critical machine tool components. The analysis was performed on standardized test specimens with identical geometric configurations to establish a direct comparison of material-dependent behavioral patterns in high-speed machining applications. The results demonstrate that Ti-6Al-4V exhibits the highest natural frequencies ranging from 195.823 Hz to 5124.67 Hz across the ten modes, followed by AISI 4140 (171.797 Hz to 4924.49 Hz) and CFRP (98.432 Hz to 2841.31 Hz). The stress analysis reveals maximum values of 1.48E+12 N/m², 1.22E+12 N/m², and 7.14E+10 N/m² for Ti-6Al-4V, AISI 4140, and CFRP respectively at the tenth mode. Displacement patterns indicate that CFRP experiences the highest deflection (890-1240 mm), while Ti-6Al-4V demonstrates the most restricted displacement (312-587 mm). The research provides valuable insights into the dynamic behavior of these materials, facilitating informed material selection for various manufacturing applications and tooling designs. The findings particularly highlight the potential of CFRP as a lightweight alternative in applications where vibration damping and lower stress concentrations are desired. Utilizing CATIA for the component modeling and frequency analysis has enabled precise simulations and detailed insights into the material-specific behaviors under dynamic machining conditions. The findings provide essential data that could influence material selection in modern manufacturing processes. This research contributes to the field by offering a deeper understanding of how material properties affect the dynamic performance of manufacturing components, guiding production engineers in optimizing designs for precision and efficiency in various machining applications.

Index Terms- AISI 4140, Ti-6Al-4V, CFRP, CATIA modeling, frequency/modal analysis, displacement analysis, stress analysis, manufacturing components, high-speed machining.

I. INTRODUCTION

Background

In modern manufacturing systems and production machinery, critical components often support high-speed motors, cutting tools, and precision equipment. These components experience complex dynamic stresses during operation, making it crucial to understand their natural vibrations for optimal design. This work focuses on analyzing the natural vibrations and patterns of cantilevered components used in manufacturing equipment, examining different materials and geometries through computational methods.

Applications in Production Technology

Cantilevered components are integral to various manufacturing and production systems:

- **Machine Tool Components:** Supporting elements for cutting tools and spindles.
- **Industrial Robots:** End-effector supports and tool holders
- **Production Line Equipment:** Automated handling systems and conveyor supports
- **CNC Machine Components:** Tool changers and work piece holders
- **Precision Manufacturing:** Measurement equipment supports and sensor mounts
- **High-Speed Production Systems:** Vibration-sensitive component supports

Aim of this Work
The primary objective is to develop a comprehensive model for analyzing the dynamic response of manufacturing components under various operational conditions using advanced computer simulations. This research aims to optimize material selection and geometric configurations for enhanced production efficiency and precision.

Material Analysis for Manufacturing Components
Understanding natural frequencies is crucial in production technology, particularly in high-speed machining and precision manufacturing. The research investigates resonance phenomena in different engineering materials commonly used in manufacturing equipment, employing mathematical models and computer simulations for comparative analysis.

II. METHODOLOGY

The study employs the Euler-Bernoulli equation to determine natural frequencies of different manufacturing materials and geometries. The analysis includes:

- Theoretical frequency calculations
- FEA validation using CATIA
- Extended analysis of first 10 natural frequencies
- Displacement analysis under various loading conditions

Engineering Materials in Manufacturing
Focus on materials commonly used in production equipment:

- **AISI 4140 Alloy Steel:** High-strength applications
- **Ti-6Al-4V:** Precision components
- **Advanced Composites:** Lightweight tooling
- **High-Speed Steel:** Cutting tool supports
- **Specialized Alloys:** Custom manufacturing applications

III. LITERATURE REVIEW

Literature on Material Analysis and Dynamic Behavior
[1] Yoo & Shin (1998) developed equations for analyzing rotating components, particularly relevant for machine tool applications.

Their work demonstrated that coupling effects become more significant at higher rotating speeds, crucial for high-speed machining applications.[2] Sina et al. (2009) introduced analysis methods for functionally graded materials, showing their potential in manufacturing applications where varying material properties are desired. Their research provides insights into shear deformation and natural frequencies essential for machine tool design. [3] Ebrahimi & Dabbagh (2019) investigated thermo-mechanical characteristics of multi-scale hybrid composites, focusing on carbon fiber and carbon nanotube reinforcements. Their findings are particularly relevant for advanced manufacturing equipment operating under varying thermal conditions.

Advanced Manufacturing Materials and Analysis
[4] Wattanasakulpong et al. (2012) studied layered functionally graded materials using experimental validation, providing valuable insights for manufacturing process optimization. Their work demonstrated the importance of material composition and boundary conditions in dynamic performance. [5] Yashavantha Kumar & Sathish Kumar (2017) analyzed smart composite materials with embedded piezoelectric elements, particularly relevant for precision manufacturing and process monitoring applications.

Dynamic Analysis in Manufacturing Systems
[6] Chouvion (2019) presented wave propagation analysis for structures with localized nonlinearities, applicable to manufacturing equipment analysis. The method offers advantages over traditional finite element approaches for analyzing machine tool components. [7] Sapountzakis & Mokos (2007) developed comprehensive 3D analysis methods for composite elements, particularly valuable for complex manufacturing equipment design. Their work addresses warping and shear deformation effects crucial in high-precision machinery.

Computational Methods in Production Analysis
[8] Fotouhi (2007) investigated flexible component analysis using finite element methods, particularly relevant for automated manufacturing systems and robotic applications.
[9] Ghafari & Rezaeepazhand (2016) presented analysis methods for rotating composite structures, essential for high-speed manufacturing equipment design. Their work specifically addresses the effects of rotational speed on component behavior.

Manufacturing Process Optimization
[10] Mehmood et al. (2014) analyzed dynamic responses under moving loads, applicable to manufacturing processes involving moving components. Their research provides insights into optimizing process parameters for dynamic loading conditions.

Material Selection and Performance Analysis
[11] Sayyad & Ghugal (2017) provided a comprehensive review of composite material applications, focusing on structural integrity and performance characteristics crucial for manufacturing equipment design. [12] Mazanoglu et al. (2009) developed methods for analyzing components with multiple discontinuities, relevant for manufacturing process optimization and tool design.

Thermal Effects in Manufacturing
[13] Avsec & Oblak (2007) studied thermal effects on component vibrations, particularly important for high-speed

machining and thermal manufacturing processes. Their work demonstrates the significant impact of temperature on material behavior during manufacturing operations.

Vibration Analysis of Advanced Materials and Structures
Functionally Graded Materials (FGMs)
[14] Wattanasakulpong and Ungbhakorn (2014) conducted pioneering research on the vibration characteristics of FGM beams with porosities. Their findings revealed that:

- The presence of porosities significantly influences both linear and nonlinear vibration responses
- Material property distribution and spring constants play crucial roles in determining frequency responses
- Nonlinear frequency ratios increase with porosity volume fraction
- Different porosity distribution patterns across beam thickness yield varying vibration characteristics

[15] Sharma and Singh (2021) employed the generalized differential quadrature (GDQ) method to analyze axially functionally graded beams. Their research demonstrated that:

- Natural frequencies vary with beam length and volume fraction index
- For shorter beams (0.5-1m), frequencies decrease with increasing volume fraction index
- Longer beams (10m) exhibit increasing frequencies with volume fraction index up to a certain threshold

Advanced Composite Materials
[16] Xu et al. (2021) investigated FG-CNT reinforced composite beams, providing valuable insights into:

- Temperature effects on natural frequencies across various boundary conditions
- Relationship between rotating speed and frequency response
- Impact of boundary stiffness on vibration characteristics
- Influence of beam slenderness and hub ratio on dynamic behaviour

Self-Healing Materials
[17] Alebrahim et al. (2015) presented groundbreaking research on self-healing hybrid composite beams, incorporating:

- Shape Memory Alloy (SMA) wire reinforcement for strain recovery
- Analysis of crack healing mechanisms
- Optimization of SMA volume fraction for maximum healing efficiency Key findings include:
- 2.5% SMA volume fraction achieves optimal healing performance
- 15% SMA volume fraction increases natural frequency by 9.6%
- Significant reduction in crack tip stress intensity factor

Analytical Methods and Computational Techniques
Advanced Numerical Methods
[18] Yu et al. (2010) developed a multivariable hierarchical finite element method that:

- Employs shifted Legendre polynomials for interpolation.
- Eliminates the need for stress-strain relations.
- Achieves high accuracy for both displacement and force fields.
- Demonstrates excellent convergence characteristics. [19] Wang et al.

(2004) introduced an innovative differential quadrature element method (DQEM) featuring:

- Enhanced computational efficiency.
- Improved boundary condition implementation.
- Superior stability for two-dimensional problems.
- Combination of DQM accuracy with FEM versatility

Probabilistic Analysis
[20] Cheng and Xiao (2007) presented a stochastic finite-element approach that:

- Incorporates uncertainties in structural parameters.
- Combines response surface methodology with Monte Carlo simulation.
- Evaluates the impact of geometric properties on frequency response.
- Analyzes the effects of axial forces on vibration characteristics

Boundary Conditions and External Influences
Boundary Condition Effects
[21] Chalah-Rezgui et al. (2014) analyzed beam vibrations under various end restraints, demonstrating:

- Relationship between support conditions and natural frequencies.
- Impact of overhang length on vibration characteristics.
- Influence of support locations on modal parameters.
- Correlation between end restraints and frequency response.

External Force Effects
[22] Liu and Chang (2005) investigated the combined effects of:

- Transverse magnetic fields.
- Axial loads.
- External forces Their research revealed that magnetic fields reduce both beam deflection and natural frequencies, with implications for various engineering applications.

Structural Health Monitoring
Crack Detection and Analysis
[23] Vigneshwaran and Behera (2014) studied beams with multiple breathing cracks, finding that:

- Crack presence significantly alters stiffness and natural frequency.
- Crack position can be identified through mode shape deviation.
- Frequency response function varies with structural integrity. 4. Relative crack depth inversely correlates with natural frequencies

Research Gaps

Based on the comprehensive literature review presented, several significant research gaps have been identified in the field of production technology:

Integration of Smart Materials and Manufacturing Processes:

- Limited research on real-time monitoring systems using smart materials in manufacturing equipment.
- Need for comprehensive studies on piezoelectric element integration in high-speed machining.
- Lack of standardized approaches for implementing self-healing materials in production systems

Thermal and Dynamic Analysis:

- Insufficient studies on combined thermo-mechanical effects in multi-scale hybrid composites under manufacturing conditions.
- Limited research on thermal behavior of FGMs in high-speed machining applications.
- 3.Need for comprehensive analysis of temperature effects on smart material performance in manufacturing processes

Advanced Material Applications:

- Gap in understanding the long-term performance of functionally graded materials in manufacturing equipment.
- Limited research on porosity effects in advanced materials under dynamic manufacturing conditions.
- Need for studies on optimal CNT reinforcement in composite materials for specific manufacturing applications

Computational Methods:

- Limited development of efficient numerical methods for real-time analysis of manufacturing processes.
- Need for improved modeling techniques for complex geometries in production equipment.
- Gap in integrating multiple analysis methods for comprehensive system evaluation

Manufacturing Process Optimization

- Insufficient research on dynamic response optimization for high-speed manufacturing processes.
- Limited studies on the relationship between material properties and manufacturing precision.
- Need for comprehensive analysis of moving load effects in automated manufacturing systems

Structural Health Monitoring:

- Gap in developing integrated health monitoring systems for manufacturing equipment.
- Limited research on crack propagation in advanced materials under manufacturing conditions
- Need for real-time damage detection methods in production systems.

IV. MODELING AND SIMULATION

Modeling of Cantilever Beam:

Figure 1 shows the model of cantilever beam with beam dimensions 50mm×50mm×500mm using Catia V5R12

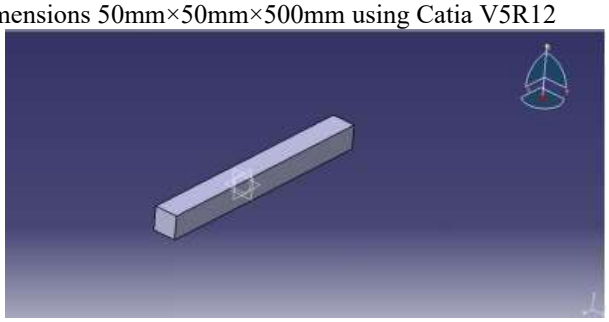

Figure 1 Beam Model

Figure 2 represents the model of cantilever beam with AISI 4140 ally steel as beam material.

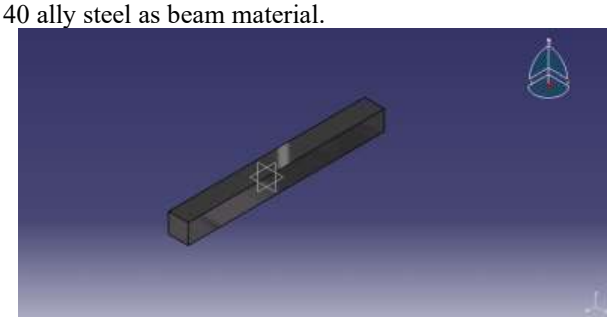

Figure 2 with AISI 4140 ally steel as Beam Material

Figure 3 represents the model of cantilever beam with Ti-6Al-4V titanium alloy as beam material.

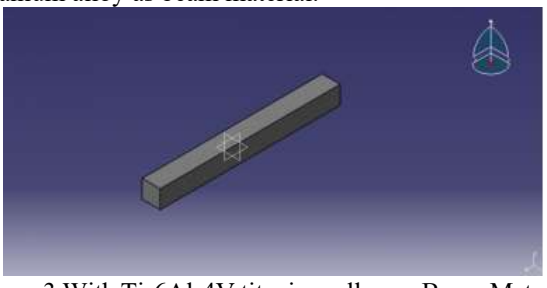

Figure 3 With Ti-6Al-4V titanium alloy as Beam Material

Figure 4 represents the model of cantilever beam with Carbon fiber reinforced polymer (CFRP) as beam material.

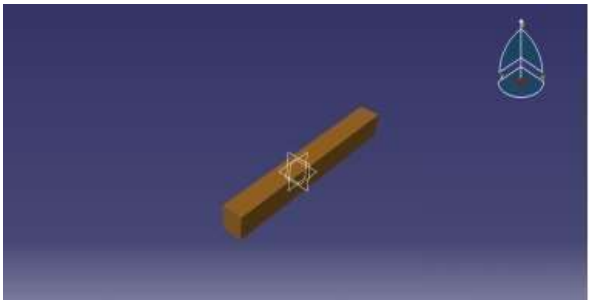

Figure 4: With Carbon fiber reinforced polymer (CFRP) Material

Figure 5 represents the model of cantilever beam with after mashing here we have used octree tetrahedron meshing with mesh size 5mm for cantilever beam model.

Figure 3.5: Meshed View

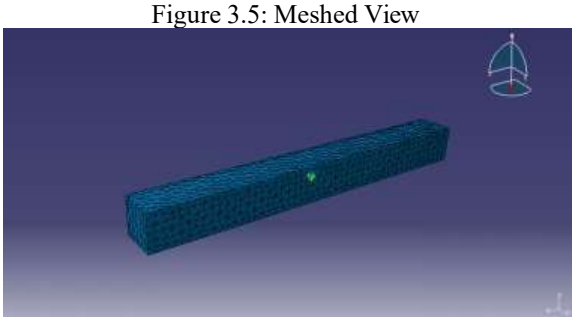

Figure 6 represents the model of cantilever beam after providing boundary condition we have taken one end fixed by using clamp command in Catia software.

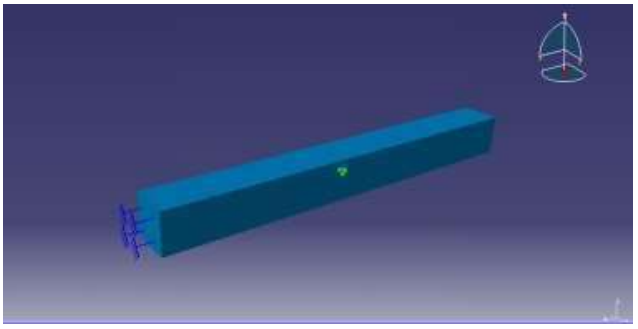

Figure 6 Applying Boundary Condition

Figure 7 represents the model of cantilever beam with application of load case here for frequency analysis we have taken frequency case with number of modes as 10 and method used is iterative subspace method for load calculation.

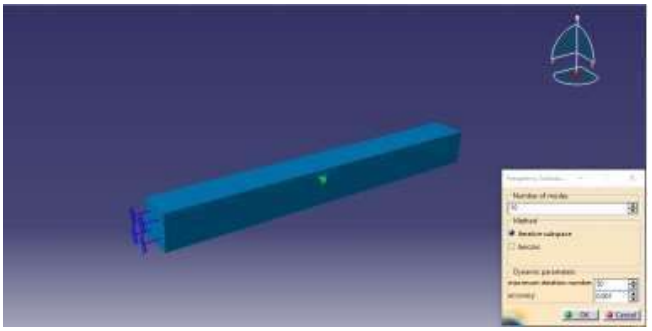

Figure 7 Applying Frequency case for cantilever beam model

Figure 8 represents the 1st mode shape and displacement value obtained for 1st modal frequency of 112.25 Hz is 1180 mm using Ti-6Al-4V titanium alloy as beam material.

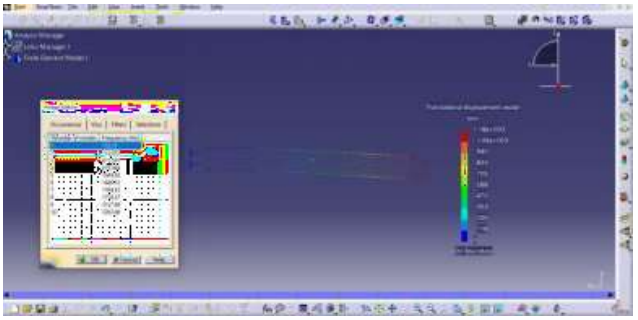

Figure.8 Displacement for First Modal Frequency of Ti-6Al-4V titanium alloy Beam

Figure 9 represents the 2nd mode shape and displacement value obtained for 2nd modal frequency of 112.931 Hz is 1170 mm using Ti-6Al-4V titanium alloy as beam material.

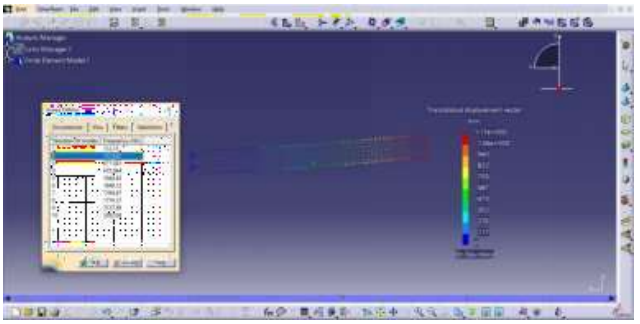

Figure 9 Displacement for Second Modal Frequency of Ti-6Al-4V titanium alloy Beam

Figure 10 represents the 3rd mode shape and displacement value obtained for 3rd modal frequency of 671.591 Hz is 1190 mm using Ti-6Al-4V titanium alloy as beam material.

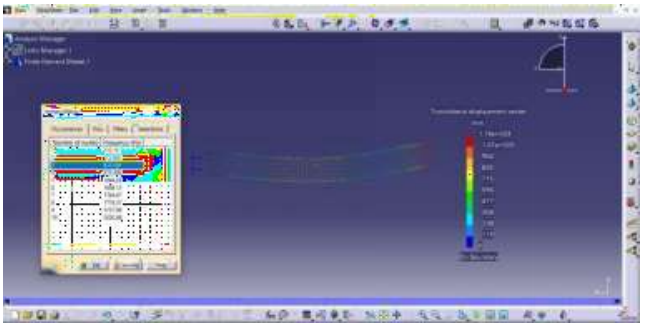

Figure 10 Displacement for Third Modal Frequency of Ti-6Al-4V titanium alloy Beam

Figure 11 represents the 4th mode shape and displacement value obtained for 4th modal frequency of 675.944 Hz is 1190 mm using Ti-6Al-4V titanium alloy as beam material.

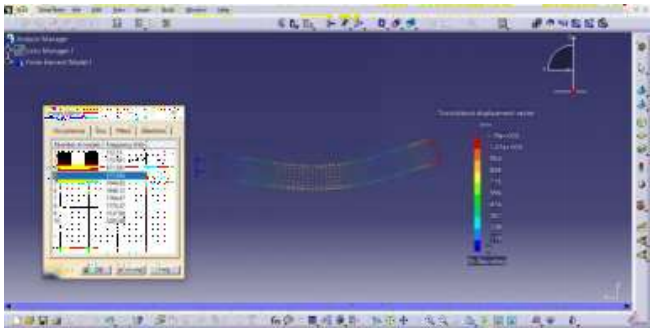

Figure 11 Displacement for Fourth Modal Frequency of Ti-6Al-4V titanium alloy Beam

Figure 12 represents the 5th mode shape and displacement value obtained for 5th modal frequency of 1044.83 Hz is 1440 mm using Ti-6Al-4V titanium alloy as beam material.

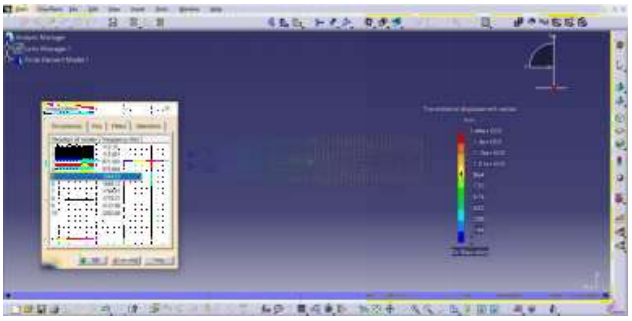

Figure 12 Displacement for Fifth Modal Frequency of Ti-6Al-4V titanium alloy Beam

Figure 13 represents the 6th mode shape and displacement value obtained for 6th modal frequency of 1648.12 Hz is 833 mm using Ti-6Al-4V titanium alloy as beam material.

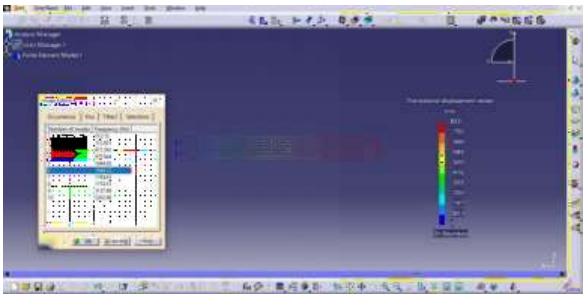

Figure 13 Displacement for Sixth Modal Frequency of Ti-6Al-4V titanium alloy Beam

Figure 14 represents the 7th mode shape and displacement value obtained for 7th modal frequency of 1764.67.25 Hz is 1220 mm using Ti-6Al-4V titanium alloy as beam material.

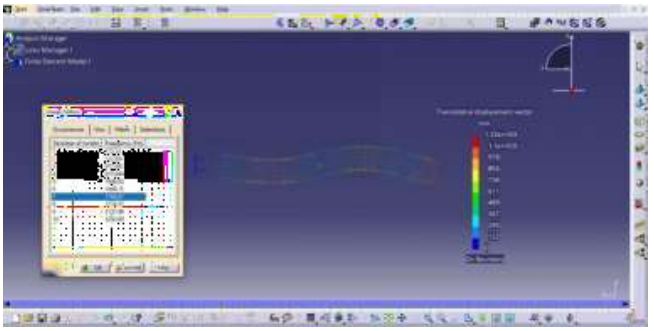

Figure 14 Displacement for Seventh Modal Frequency of Ti-6Al-4V titanium alloy Beam

Figure 15 represents the 8th mode shape and displacement value obtained for 8th modal frequency of 1774.37 Hz is 1220 mm using Ti-6Al-4V titanium alloy as beam material.

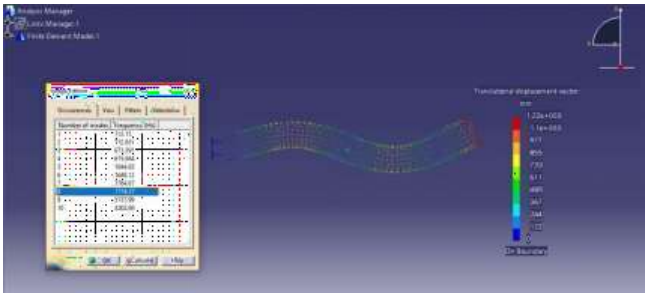

Figure 15 Displacement for Eighth Modal Frequency of Ti-6Al-4V titanium alloy Beam

Figure 16 represents the 9th mode shape and displacement value obtained for 9th modal frequency of 3137.99 Hz is 1450 mm using Ti-6Al-4V titanium alloy as beam material.

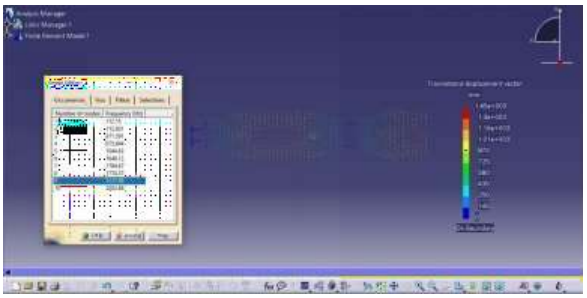

Figure 16 Displacement for Ninth Modal Frequency of Ti-6Al-4V titanium alloy Beam

Figure 17 represents the 10th mode shape and displacement value obtained for 10th modal frequency of 3202 Hz is 1270 mm using Ti-6Al-4V titanium alloy as beam material.

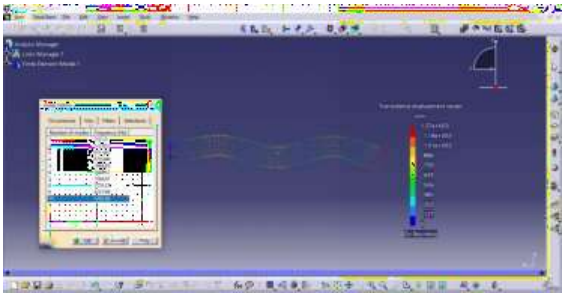

Figure 3.17 Displacement for Tenth Modal Frequency of Ti-6Al-4V titanium alloy Beam

Figure 18 represents the 1st mode shape and stress value obtained for 1st modal frequency of 112.15 Hz is 1.34E+10 N/m2 using Ti-6Al-4V titanium alloy as beam material.

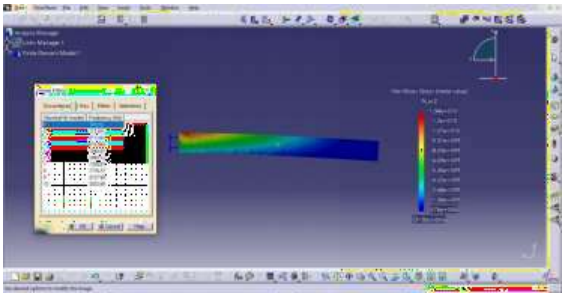

Figure 18 Stress Value for First Modal Frequency of Ti-6Al-4V titanium alloy Beam

Figure 19 represents the 2nd mode shape and stress value obtained for 2nd modal frequency of 112.931 Hz is 1.28E+10 N/m2 using Ti-6Al-4V titanium alloy as beam material.

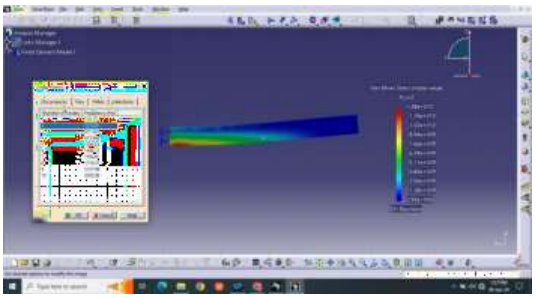

Figure 19 Stress Value for Second Modal Frequency of Ti-6Al-4V titanium alloy Beam

Figure 20 represents the 3rd mode shape and stress value obtained for 3rd modal frequency of 671.591 Hz is 7.27E+10 N/m2 using Ti-6Al-4V titanium alloy as beam material.

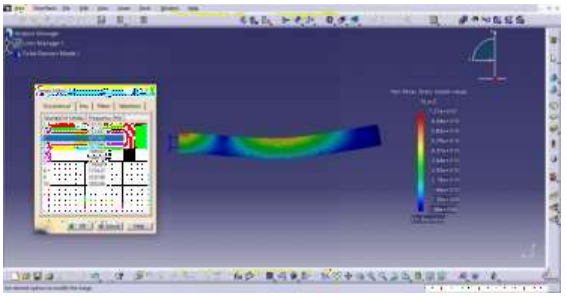

Figure 20 Stress Value for Third Modal Frequency of Ti-6Al-4V titanium alloy Beam

Figure 21 represents the 4th mode shape and stress value obtained for 4th modal frequency of 675.944 Hz is 6.95E+10 N/m2 using Ti-6Al-4V titanium alloy as beam material.

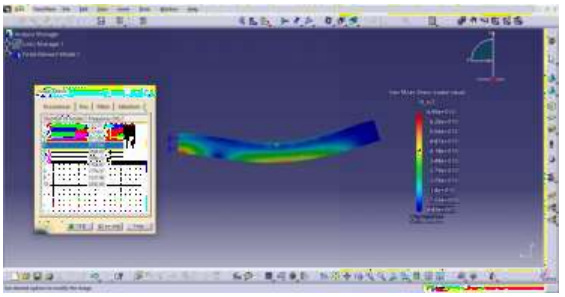

Figure 21 Stress Value for Fourth Modal Frequency of Ti-6Al-4V titanium alloy Beam

Figure 22 represents the 5th mode shape and stress value obtained for 5th modal frequency of 1044.83 Hz is 6.94E+10 N/m2 using Ti-6Al-4V titanium alloy as beam material.

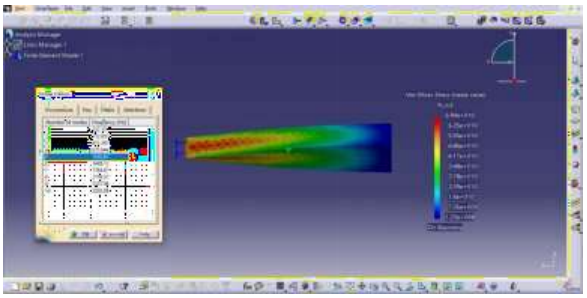

Figure.22 Stress Value for Fifth Modal Frequency of Ti-6Al-4V titanium alloy Beam

Figure 3.23 represents the 6th mode shape and stress value obtained for 6th modal frequency of 1648.12 Hz is 6.64E+10 N/m2 using Ti-6Al-4V titanium alloy as beam material.

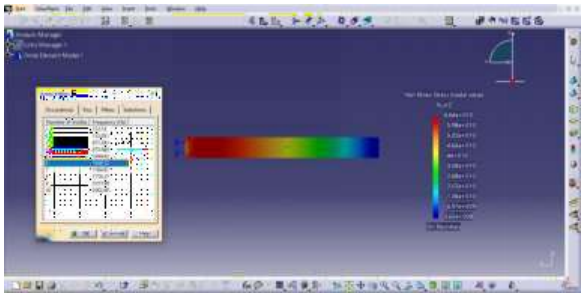

Figure 23 Stress Value for Sixth Modal Frequency of Ti-6Al-4V titanium alloy Beam

Figure 24 represents the 7th mode shape and stress value obtained for 7th modal frequency of 1764.67 Hz is 1.7E+11 N/m2 using Ti-6Al-4V titanium alloy as beam material.

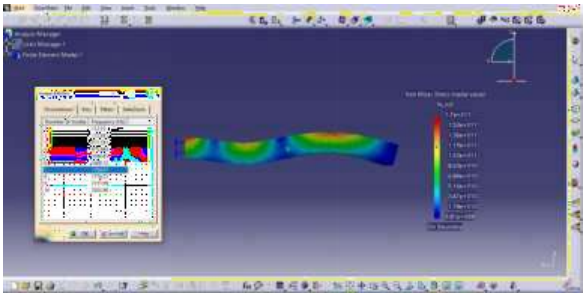

Figure 24 Stress Value for Seventh Modal Frequency of Ti-6Al-4V titanium alloy Beam

Figure.25 represents the 8th mode shape and stress value obtained for 8th modal frequency of 1774.67 Hz is 1.74E+11 N/m2 using Ti-6Al-4V titanium alloy as beam material.

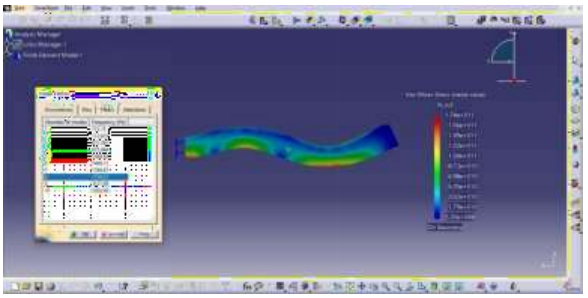

Figure.25 Stress Value for Eighth Model Frequency of Ti-6Al-4V titanium alloy Beam

Figure 26 represents the 9th mode shape and stress value obtained for 9th modal frequency of 3137.99 Hz is 2.1E+11 N/m2 using Ti-6Al-4V titanium alloy as beam material.

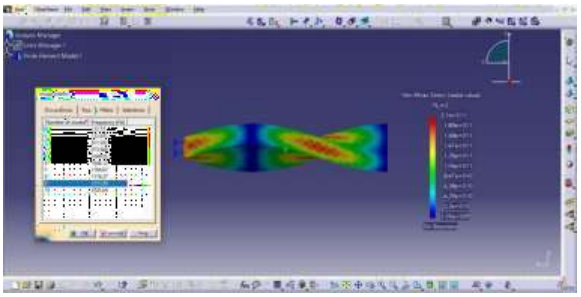

Figure 26 Stress Value for Ninth Modal Frequency of Ti-6Al-4V titanium alloy Beam

Figure 27 represents the 10th mode shape and stress value obtained for 10th modal frequency of 3202.69 Hz is 2.78E+11 N/m2 using Ti-6Al-4V titanium alloy as beam material.

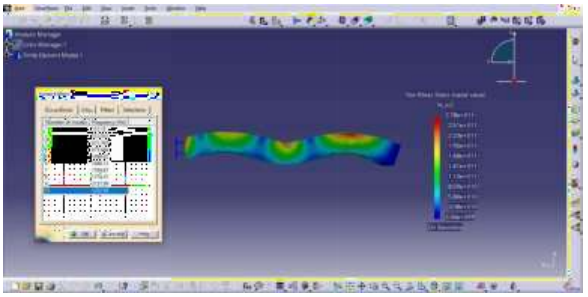

Figure 27 Stress Value for Tenth Modal Frequency of Ti-6Al-4V titanium alloy Beam

Figure 28 represents the 1st mode shape and displacement value obtained for 1st modal frequency of 171.797 Hz is 638 mm using AISI 4140 ally steel as beam material.

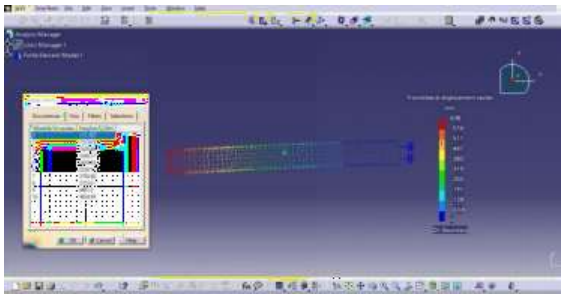

Figure 28 Displacement for First Modal Frequency of AISI 4140 ally steel Beam

Figure 29 represents the 2nd mode shape and displacement value obtained for 2nd modal frequency of 172.819 Hz is 638 mm using AISI 4140 ally steel as beam material.

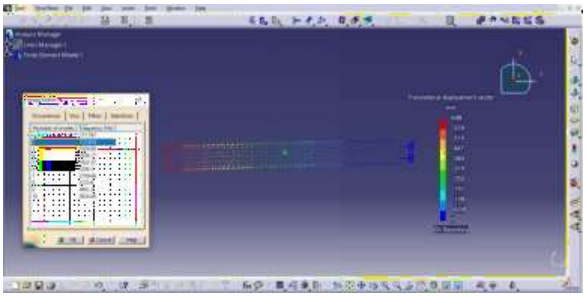

Figure 29 Displacement for Second Modal Frequency of AISI 4140 ally steel Beam

Figure 30 represents the 3rd mode shape and displacement value obtained for 3rd modal frequency of 1029.86 Hz is 648 mm using AISI 4140 ally steel as beam material.

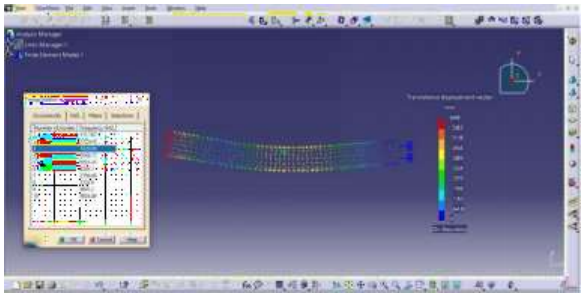

Figure 30 Displacement for Third Modal Frequency of AISI 4140 ally steel Beam

Figure 31 represents the 4th mode shape and displacement value obtained for 4th modal frequency of 1036.17 Hz is 647 mm using AISI 4140 ally steel as beam material.

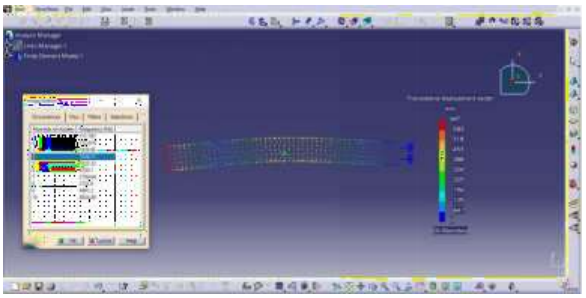

Figure 31 Displacement for Fourth Modal Frequency of AISI 4140 ally steel Beam

Figure 32 represents the 5th mode shape and displacement value obtained for 5th modal frequency of 1625.33 Hz is 782 mm using AISI 4140 ally steel as beam material.

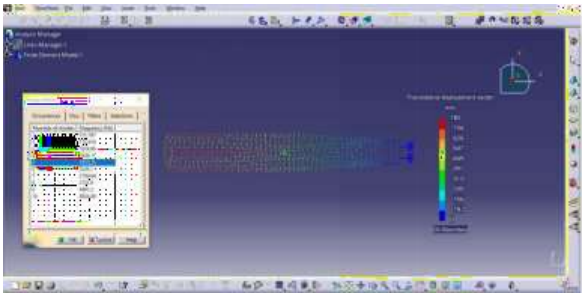

Figure 32 Displacement for Fifth Modal Frequency of AISI 4140 ally steel Beam

Figure 33 represents the 6th mode shape and displacement value obtained for 6th model frequency of 2530.1 Hz is 452 mm using AISI 4140 ally steel as beam material.

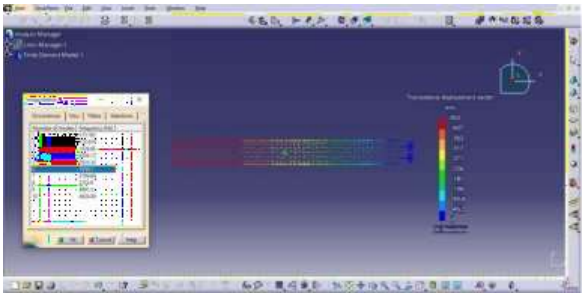

Figure 33 Displacement for Sixth Modal Frequency of AISI 4140 ally steel Beam

Figure 34 represents the 7th mode shape and displacement value obtained for 7th model frequency of 2709.69 Hz is 665 mm using AISI 4140 ally steel as beam material.

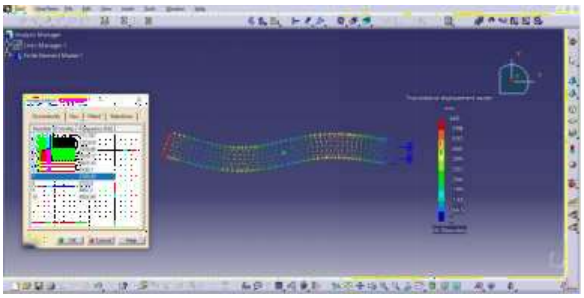

Figure 34 Displacement for Seventh Modal Frequency of AISI 4140 ally steel Beam

Figure.35 represents the 8th mode shape and displacement value obtained for 8th model frequency of 2723.9 Hz is 664 mm using AISI 4140 ally steel as beam material.

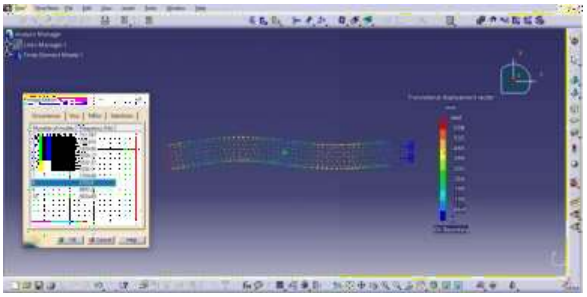

Figure 35 Displacement for Eighth Modal Frequency of AISI 4140 ally steel Beam

Figure 36 represents the 9th mode shape and displacement value obtained for 9th model frequency of 4881.2 Hz is 793 mm using AISI 4140 ally steel as beam material.

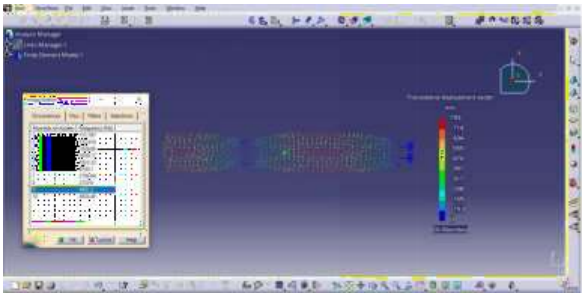

Figure 36 Displacement for Ninth Modal Frequency of AISI 4140 ally steel Beam

Figure37 represents the 10th mode shape and displacement value obtained for 10th model frequency of 4924.49 Hz is 691 mm using AISI 4140 ally steel as beam material.

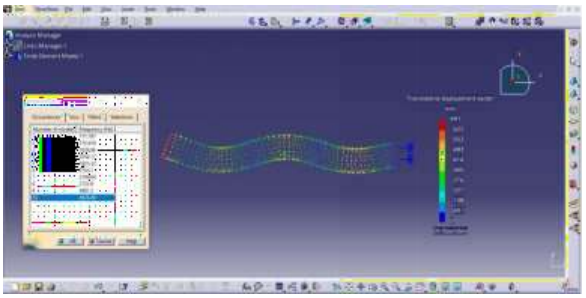

Figure 37 Displacement for Tenth Modal Frequency of AISI 4140 ally steel Beam

Figure 38 represents the 1st mode shape and stress value obtained for 1st modal frequency of 171.797 Hz is 5.9E+10 N/m2 using AISI 4140 ally steel as beam material.

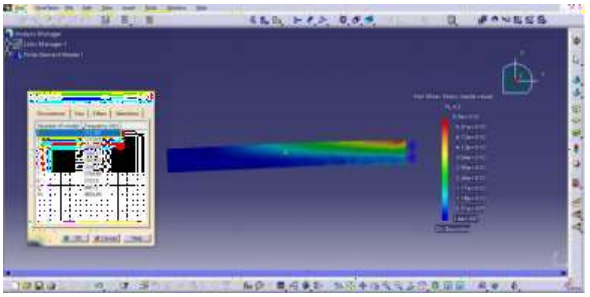

Figure 38 Stress Value for First Modal Frequency of AISI 4140 ally steel Beam

Figure 39 represents the 2nd mode shape and stress value obtained for 2nd modal frequency of 172.919 Hz is 5.54E+10 N/m2 using AISI 4140 ally steel as beam material.

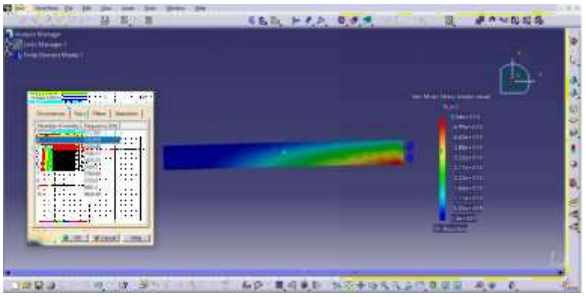

Figure 39 Stress Value for Second Modal Frequency of AISI 4140 ally steel Beam

Figure 40 represents the 3rd mode shape and stress value obtained for 3rd modal frequency of 1029.86 Hz is 3.21E+11 N/m2 using AISI 4140 ally steel as beam material.

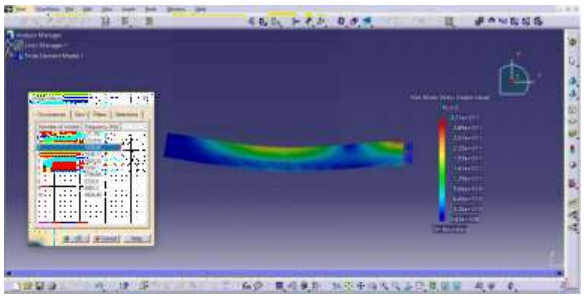

Figure .40 Stress Value for Third Modal Frequency of AISI 4140 ally steel Beam

Figure.41 represents the 4th mode shape and stress value obtained for 4th modal frequency of 1036.17 Hz is 3.21E+11 N/m2 using AISI 4140 ally steel as beam material.

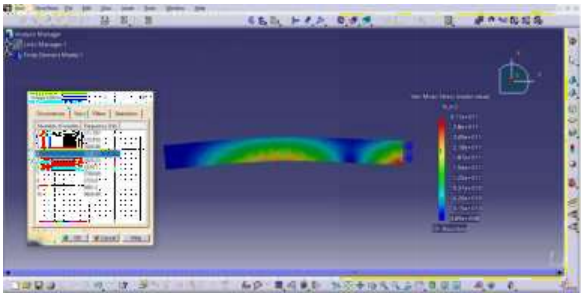

Figure 41 Stress Value for Fourth Modal Frequency of AISI 4140 ally steel Beam

Figure.42 represents the 5th mode shape and stress value obtained for 5th modal frequency of 1625.33 Hz is 3.11E+11 N/m2 using AISI 4140 ally steel as beam material.

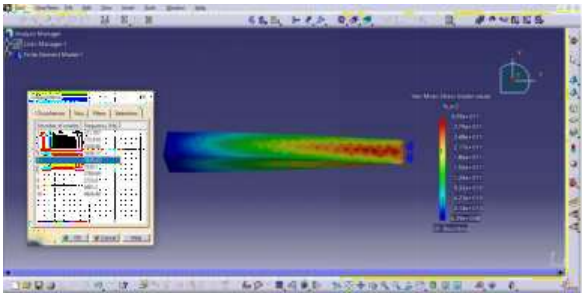

Figure 42 Stress Value for Fifth Modal Frequency of AISI 4140 ally steel Beam

Figure 43 represents the 6th mode shape and stress value obtained for 6th modal frequency of 2530.1 Hz is 2.91E+11 N/m2 using AISI 4140 ally steel as beam material.

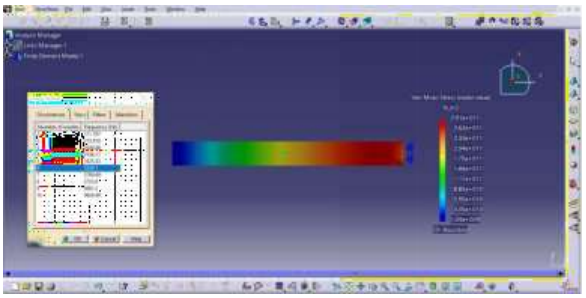

Figure 43 Stress Value for Sixth Modal Frequency of AISI 4140 ally steel Beam

Figure 44 represents the 7th mode shape and stress value obtained for 7th modal frequency of 2709.69 Hz is 7.5E+11 N/m2 using AISI 4140 ally steel as beam material.

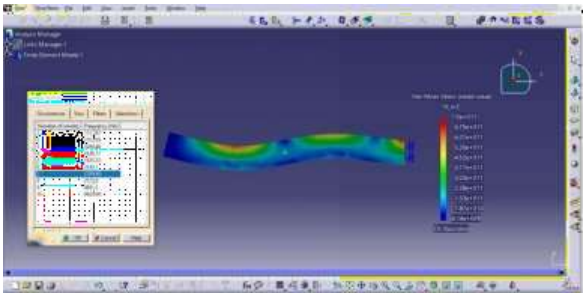

Figure 44 Stress Value for Seventh Modal Frequency of AISI 4140 ally steel Beam

Figure 45 represents the 8th mode shape and stress value obtained for 8th modal frequency of 2723.9 Hz is 7.78E+11 N/m2 using AISI 4140 ally steel as beam material.

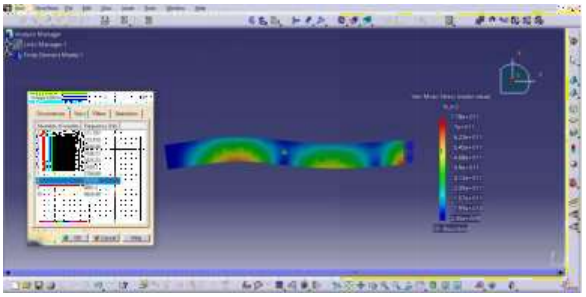

Figure 45 Stress Value for Eighth Model Frequency of AISI 4140 ally steel Beam

Figure 46 represents the 9th mode shape and stress value obtained for 9th modal frequency of 4881.2 Hz is 9.42E+11 N/m2 using AISI 4140 ally steel as beam material.

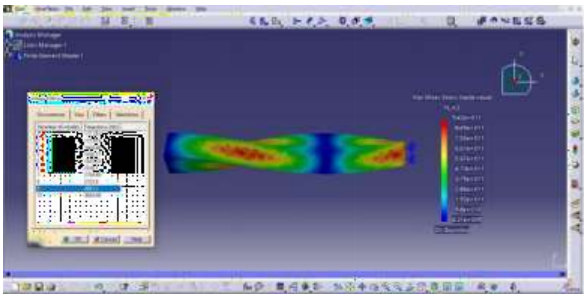

Figure 46 Stress Value for Ninth Modal Frequency of AISI 4140 ally steel Beam

Figure 47 represents the 10th mode shape and stress value obtained for 10th modal frequency of 4924.49 Hz is 1.22E+11 N/m2 using AISI 4140 ally steel as beam material.

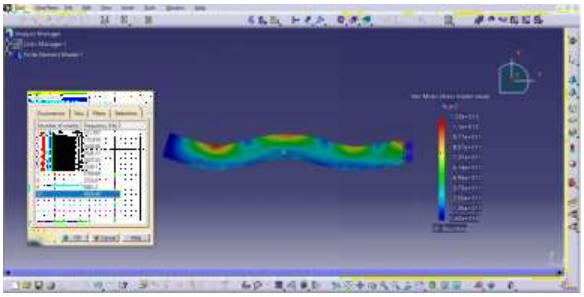

Figure 47 Stress Value for Tenth Modal Frequency of AISI 4140 ally steel Beam

Figure 48 represents the 1st mode shape and displacement value obtained for 1st model frequency of 50.7722 Hz is 1570 mm using carbon fiber reinforced polymer (CFRP) as beam material.

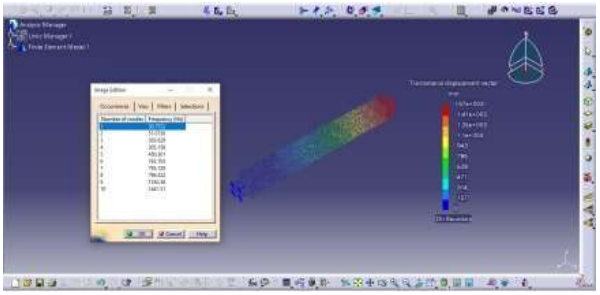

Figure 48 Displacement for First Modal Frequency of Carbon fiber reinforced polymer (CFRP) Beam

Figure 49 represents the 2nd mode shape and displacement value obtained for 2nd model frequency of 51.0736 Hz is 1570 mm using carbon fiber reinforced polymer (CFRP) as beam material.

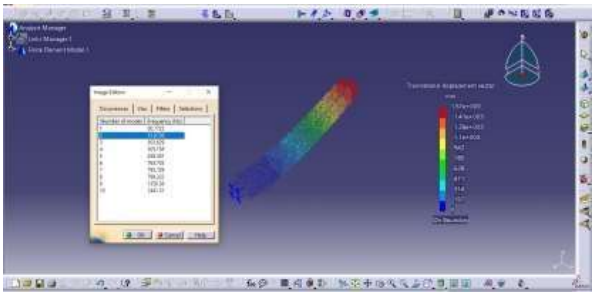

Figure 49 Displacement for Second Modal Frequency of Carbon fiber reinforced polymer (CFRP) Beam

Figure 50 represents the 3rd mode shape and displacement value obtained for 3rd model frequency of 303.629 Hz is 1600 mm using carbon fiber reinforced polymer (CFRP) as beam material.

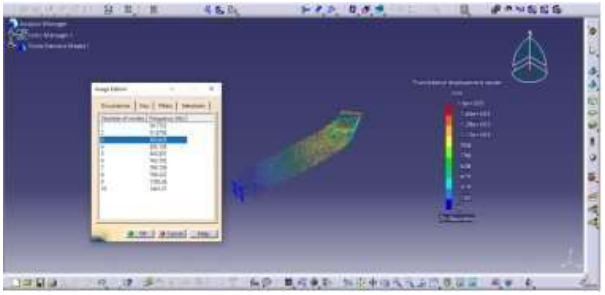

Figure 50 Displacement for Third Modal Frequency of Carbon fiber reinforced polymer (CFRP) Beam

Figure 51 represents the 4th mode shape and displacement value obtained for 4th model frequency of 305.158 Hz is 1600 mm using carbon fiber reinforced polymer (CFRP) as beam material.

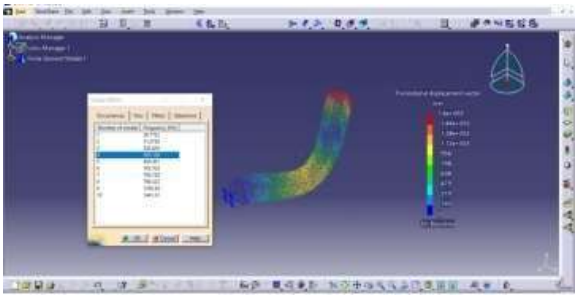

Figure 51 Displacement for Fourth Modal Frequency of Carbon fiber reinforced polymer (CFRP) Beam

Figure 52 represents the 5th mode shape and displacement value obtained for 5th model frequency of 450.301 Hz is 1920 mm using carbon fiber reinforced polymer as beam material.

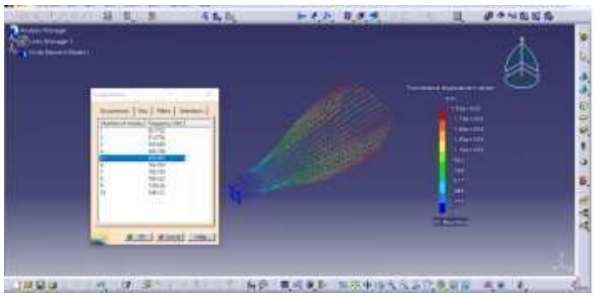

Figure 52 Displacement for Fifth Modal Frequency of Carbon fiber reinforced polymer (CFRP) Beam

Figure 53 represents the 6th mode shape and displacement value obtained for 6th model frequency of 763.703 Hz is 1110 mm using carbon fiber reinforced polymer as beam material.

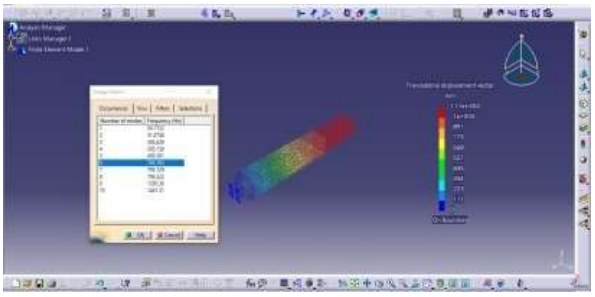

Figure 53 Displacement for Sixth Modal Frequency of Carbon fiber reinforced polymer (CFRP) Beam

Figure 54 represents the 7th mode shape and displacement value obtained for 7th model frequency of 795.729 Hz is 1640 mm using carbon fiber reinforced polymer as beam material.

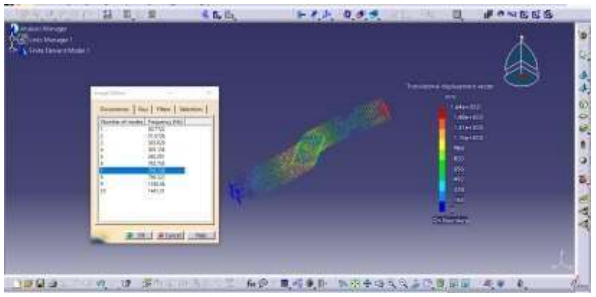

Figure 54 Displacement for Seventh Modal Frequency of Carbon fiber reinforced polymer (CFRP) Beam

Figure 55 represents the 8th mode shape and displacement value obtained for 8th model frequency of 799.322 Hz is 1640 mm using carbon fiber reinforced polymer as beam material.

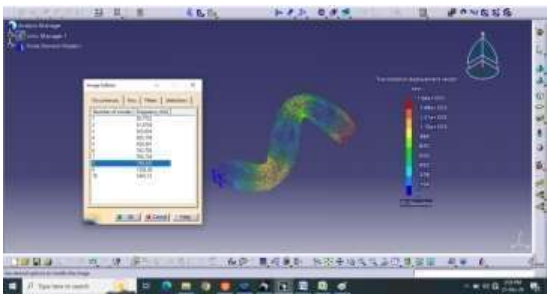

Figure 55 Displacement for Eighth Modal Frequency of Carbon fiber reinforced polymer (CFRP) Beam

Figure 56 represents the 9th mode shape and displacement value obtained for 9th model frequency of 1350.36 Hz is 1940 mm using carbon fiber reinforced polymer as beam material.

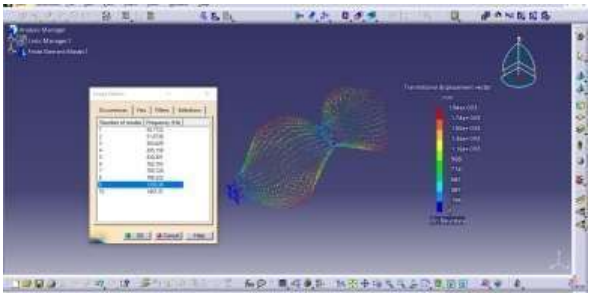

Figure 56 Displacement for Ninth Modal Frequency of Carbon fiber reinforced polymer (CFRP) Beam

Figure 57 represents the 10th mode shape and displacement value obtained for 10th model frequency of 1441.31 Hz is 1700 mm using carbon fiber reinforced polymer as beam material.

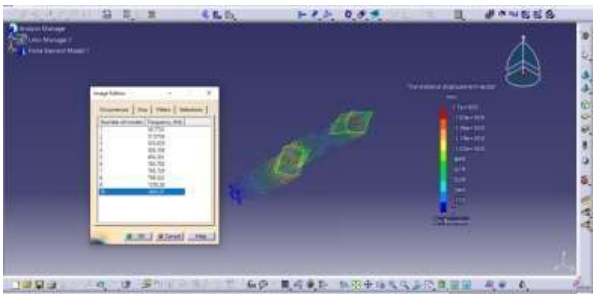

Figure 57 Displacement for Tenth Modal Frequency of Carbon fiber reinforced polymer (CFRP) Beam

Figure 58 represents the 1st mode shape and stress value obtained for 1st modal frequency of 50.7722 Hz is 2.22E+09 N/m2 using Carbon fiber reinforced polymer as beam material.

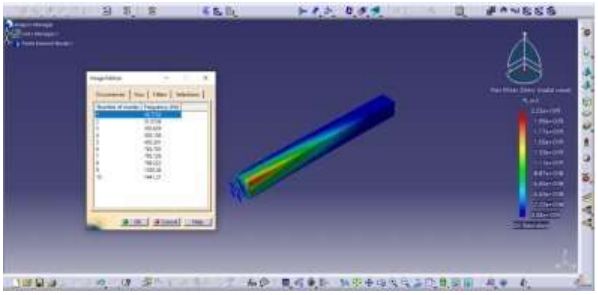

Figure 58 Stress for First Modal Frequency of Carbon fiber reinforced polymer (CFRP) Beam

Figure 59 represents the 2nd mode shape and stress value obtained for 2nd modal frequency of 51.0736 Hz is 2.19E+09 N/m2 using Carbon fiber reinforced polymer as beam material.

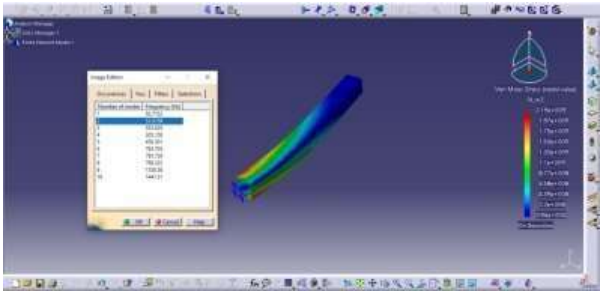

Figure 59 Stress for Second Modal Frequency of Carbon fiber reinforced polymer (CFRP) Beam

Figure 60 represents the 3rd mode shape and stress value obtained for 3rd modal frequency of 303.629 Hz is 1.27E+10 N/m2 using Carbon fiber reinforced polymer (CFRP) as beam material.

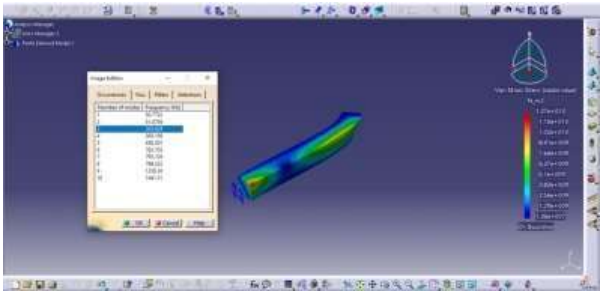

Figure 60 Stress for Third Modal Frequency of Carbon fiber reinforced polymer (CFRP) Beam

Figure 61 represents the 4th mode shape and stress value obtained for 4th modal frequency of 305.158 Hz is 1.28E+10 N/m2 using Carbon fiber reinforced polymer as beam material.

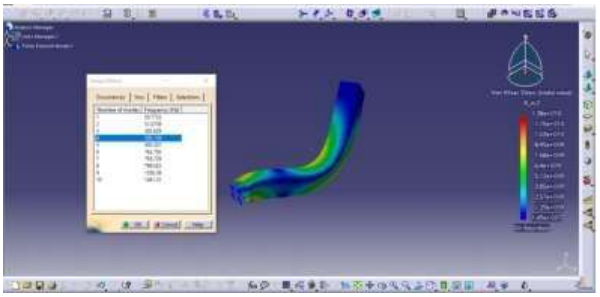

Figure 61 Stress for Fourth Modal Frequency of Carbon fiber reinforced polymer (CFRP) Beam

Figure 62 represents the 5th mode shape and stress value obtained for 5th modal frequency of 450.301 Hz is 1.1E+10 N/m2 using Carbon fiber reinforced polymer (CFRP) as beam material.

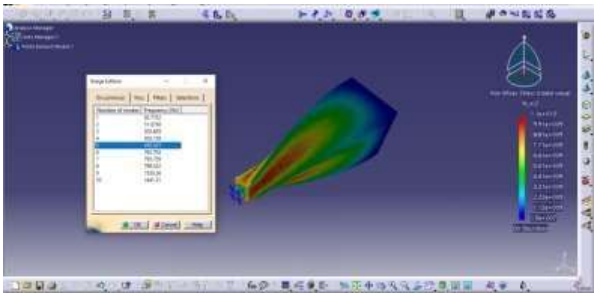

Figure 62 Stress for Fifth Modal Frequency of Carbon fiber reinforced polymer (CFRP) Beam

Figure 63 represents the 6th mode shape and stress value obtained for 6th modal frequency of 763.703 Hz is 1.27E+10 N/m2 using Carbon fiber reinforced polymer (CFRP) as beam material.

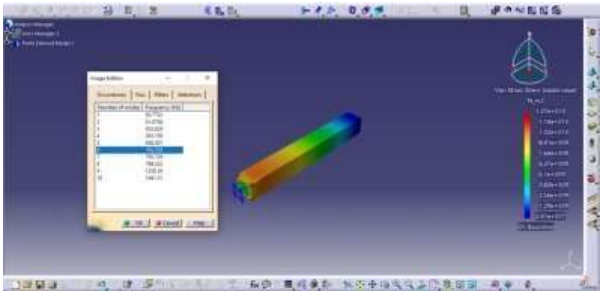

Figure 63 Stress for Sixth Modal Frequency of Carbon fiber reinforced polymer (CFRP) Beam

Figure 64 represents the 7th mode shape and stress value obtained for 7th modal frequency of 795.729 Hz is 3.1E+10 N/m2 using Carbon fiber reinforced polymer (CFRP) as beam material.

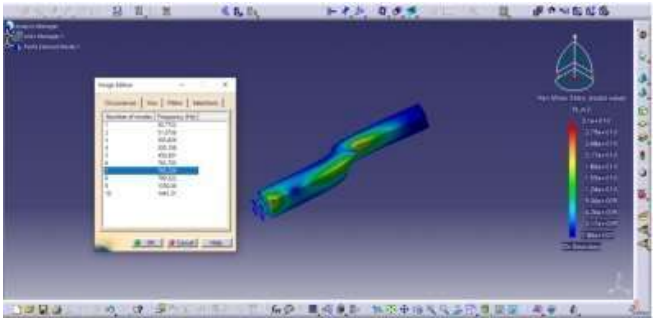

Figure 64 Stress for Seventh Modal Frequency of Carbon fiber reinforced polymer (CFRP) Beam

Figure 65 represents the 8th mode shape and stress value obtained for 8th modal frequency of 799.322 Hz is 3.24E+10 N/m2 using Carbon fiber reinforced polymer (CFRP) as beam material.

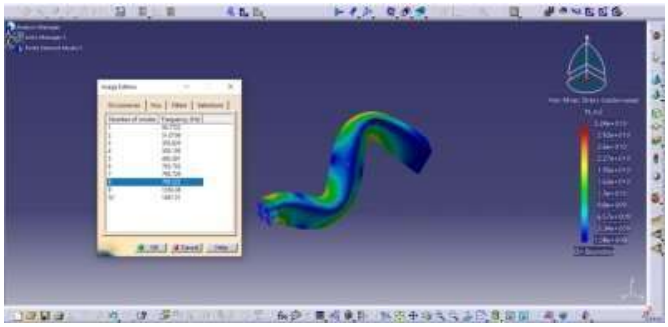

Figure 65 Stress for Eighth Modal Frequency of Carbon fiber reinforced polymer (CFRP) Beam

Figure 66 represents the 9th mode shape and stress value obtained for 9th modal frequency of 1350.36 Hz is 3.27E+10 N/m2 using Carbon fiber reinforced polymer (CFRP) as beam material.

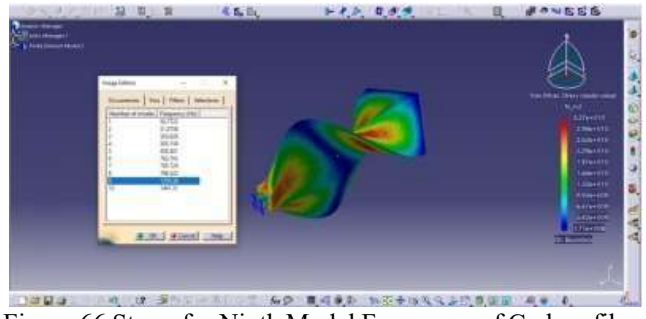

Figure 66 Stress for Ninth Modal Frequency of Carbon fiber reinforced polymer (CFRP) Beam

Figure 67 represents the 10th mode shape and stress value obtained for 10th modal frequency of 1441.31 Hz is 5.08E+10 N/m2 using Carbon fiber reinforced polymer (CFRP) as beam material.

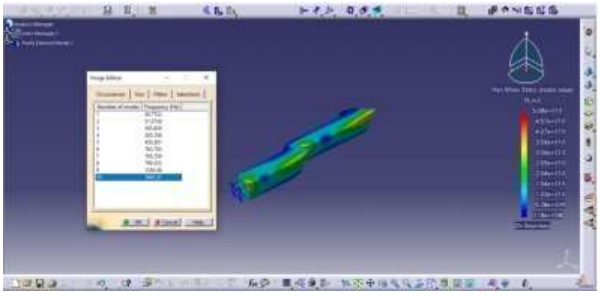

Figure 67 Stress for Tenth Modal Frequency of Carbon fiber reinforced polymer (CFRP) Beam

V. RESULTS AND DISCUSSIONS

Result Table:

Table1: Result Table for Frequency of AISI 4140 alloy steel and Ti-6Al-4V titanium alloy beams for first 10 modal frequencies

Number of Mode	Frequency (Hz) for AISI 4140 alloy steel Beam	Frequency (Hz) for Ti-6Al-4V titanium alloy Beam	Frequency (Hz) for Carbon fiber reinforced polymer Epoxy Beam
1	171.797	112.15	50.772
2	172.919	112.931	51.0736
3	1029.86	671.591	303.629
4	1036.17	675.944	305.158
5	1625.33	1044.83	450.301
6	2530.1	1648.12	763.703
7	2709.69	1764.67	795.729
8	2723.9	1774.67	799.322
9	4881.2	3137.99	1350.36
10	4924.49	3202.69	1441.31

Table2: Result Table for Stress of AISI 4140 alloy steel and Ti-6Al-4V titanium alloy beams for first 10 modal frequencies

Number of Mode	Stress for AISI 4140 alloy steel Beam (N/m2)	Stress for Ti-6Al-4V titanium alloy Beam (N/m2)	Stress for Carbon fiber reinforced polymer Beam (N/m2)
1	5.9E+10	1.34E+10	2.22E+09
2	5.54E+10	1.28E+10	2.19E+09
3	3.21E+11	7.27E+10	1.27 E+10
4	3.11E+11	6.95E+10	1.28 E+10
5	3.09E+11	6.94E+10	1.10 E+10
6	2.91E+11	6.64E+10	1.27 E+10
7	7.5E+11	1.7E+11	3.10 E+10
8	7.78E+11	1.74E+11	3.24 E+10
9	9.42E+11	2.1E+11	3.28 E+10
10	1.22E+12	2.78E+11	5.04 E+10

Table 4.3: Result Table for displacement of AISI 4140 alloy steel and Ti-6Al-4V titanium alloy beams for first 10 modal frequencies

Number of Mode	displacement for AISI 4140 alloy steel Beam (mm)	displacement for Ti-6Al-4V titanium alloy Beam (mm)	Displacement for Carbon fiber reinforced polymer Beam (mm)
1	638	1180	1570
2	638	1170	1570
3	648	1190	1600
4	647	1190	1600
5	782	1440	1920
6	452	833	1110
7	665	1220	1640
8	664	1220	1640
9	793	1450	1940
10	691	1270	1700

Result Figures:

The graph 4.1 shows the relationship between the number of modes and their corresponding frequencies for both AISI 4140 alloy steel, Ti-6Al-4V titanium alloy and CFRP alloy b

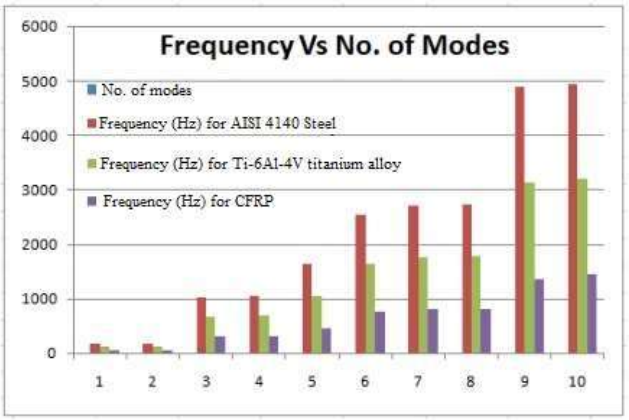

Figure 67 Graph of Frequency Vs no. of Modes for AISI 4140 alloy steel beam; Ti-6Al-4V titanium alloy and CFRP alloy Beam Materials

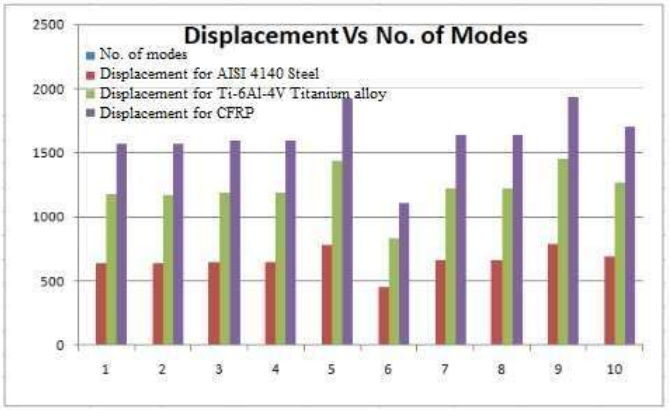

Figure 68 Graph of Displacement Vs no. of Modes for AISI 4140 alloy steel beam; Ti-6Al-4V titanium alloy Beam and CFRP Beam Materials

The graph 4.2 shows the relationship between the number of modes and their corresponding displacements values for both AISI 4140 alloy steel; Ti-6Al-4V titanium alloy and CFRP beams.

The graph 4.3 shows the relationship between the number of modes and their corresponding stress values for both AISI 4140 alloy steel, Ti-6Al-4V titanium alloy and CFRP beams.

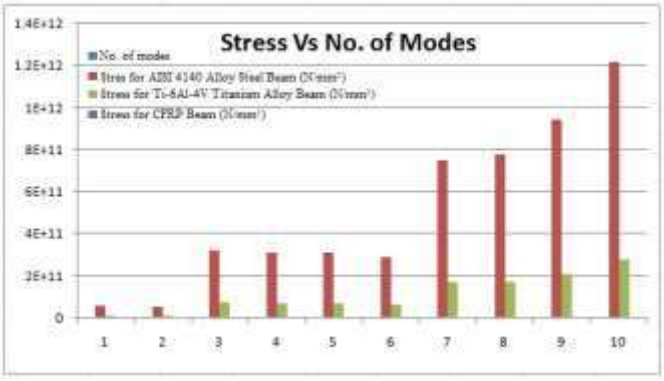

Figure 69 Graph of Stress Vs n. of Modes for AISI 4140 alloy steel; Ti-6Al-4V titanium alloy and CFRP Beams

Discussions:
The modal analysis of AISI 4140 alloy steel, Ti-6Al-4V titanium alloy, and carbon fiber reinforced polymer epoxy beams reveals several significant findings:

Frequency Analysis:
- The AISI 4140 alloy steel beam consistently exhibits the highest natural frequencies across all modes, followed by Ti-6Al-4V titanium alloy and carbon fiber reinforced polymer epoxy beams respectively.
- There is a notable pattern where frequencies increase significantly between modes 2-3 and modes 8-9 for all materials.
- The first two modes show relatively close frequency values for each material, suggesting similar vibrational behavior at lower modes.
- The AISI 4140 alloy steel beam reaches a maximum frequency of 4924.49 Hz at mode 10, while Ti-6Al-4V titanium alloy and carbon fiber reinforced polymer reach 3202.69 Hz and 1441.31 Hz respectively.

Stress Analysis:
- The stress values follow a generally increasing trend with higher modes for all materials.
- AISI 4140 alloy steel exhibits the highest stress values, reaching 1.22E+12 N/m² at mode 10.
- The Ti-6Al-4V titanium alloy beam shows intermediate stress values, with a maximum of 2.78E+11 N/m².
- Carbon fiber reinforced polymer epoxy demonstrates significantly lower stress values, peaking at 5.04E+10 N/m² at mode 10.
- The stress variation between modes is more pronounced in higher modes (7-10) compared to lower modes.

Displacement Analysis:
- Carbon fiber reinforced polymer epoxy beam shows the highest displacement values across all modes, ranging from 1570-1940 mm.
- Ti-6Al-4V titanium alloy follows with intermediate displacement values (833-1450 mm).
- AISI 4140 alloy steel beam shows the lowest displacement values (438-793 mm).
- All materials show similar patterns of displacement variation across modes, with peak displacements occurring at mode 9.

V. CONCLUSION

Based on the comprehensive modal analysis conducted, the following conclusions can be drawn:

Material Performance:
- AISI 4140 alloy steel beams demonstrate superior stiffness characteristics with highest natural frequencies but also experience the highest stress levels.
- Ti-6Al-4V titanium alloy beams offer a balanced performance with moderate frequencies and stress values.
- Carbon fiber reinforced polymer epoxy beams show the highest flexibility with lowest natural frequencies and stress values, but highest displacement.

Structural Implications:
- The significant variation in natural frequencies suggests that each material would be suitable for different applications based on operational frequencies.
- The lower stress values in carbon fiber reinforced polymer epoxy beams indicate potential advantages in applications where stress reduction is critical.
- The displacement characteristics suggest that AISI 4140 alloy steel would be most suitable for applications requiring minimal deflection.

Design Considerations:
- The modal behavior patterns observed can be valuable for preventing resonance in structural designs.
- The stress-frequency relationships established can guide material selection based on specific application requirements.

Future Scope:
The following areas can be explored for further investigation:
Material Development:
- Investigation of hybrid composites combining the advantages of multiple materials
- Development of modified carbon fiber reinforced polymer compositions to enhance frequency response while maintaining low stress characteristics

Analysis Extensions:
- Study of damping characteristics for these materials under different loading conditionsInvestigation of temperature effects on modal parameters

- Analysis of fatigue behavior under repeated modal excitation

Application-Specific Research:
Development of optimization algorithms for material selection based on specific frequency requirements
Investigation of scaling effects for different beam dimensions
Study of joint behavior and connections using these materials

Experimental Validation:
- Conduct experimental modal analysis to validate the numerical results
- Investigation of actual service conditions and their impact on modal parameters
- Study of environmental factors affecting the long-term modal behaviour

Sustainable Aspects:
- Life cycle assessment of different beam materials
- Investigation of recyclability and environmental impact
- Development of more sustainable alternatives with comparable performance characteristics.

REFERENCES

1. Yoo, J., & Shin, H. (1998). Vibration analysis of rotating cantilever beams. Journal of Sound and Vibration, 212(5), 807-828.
2. Sina, S. A., Navazi, H. M., & Haddadpour, H. (2009). An analytical method for free vibration analysis of functionally graded beams. Materials & Design, 30(3), 741-747.
3. Ebrahimi, F., & Dabbagh, A. (2019). Thermal effects on nonlinear vibration characteristics of nanocomposite beams reinforced with functionally graded multi-walled carbon nanotubes. Mechanics of Advanced Materials and Structures, 26(12), 1025-1037.
4. Wattanasakulpong, N., Prusty, B. G., & Kelly, D. W. (2012). Free and forced vibration analysis of functionally graded beams with experimental validation. Materials & Design, 36, 182-190.
5. Yashavantha Kumar, G. A., & Sathish Kumar, B. G. (2017). Design and analysis of smart composite structures with embedded piezoelectric sensors and actuators. Journal of Intelligent Material Systems and Structures, 28(20), 3025-3037.
6. Chouvion, B. (2019). Wave-based method for the structural dynamics of complex rotating machines. Journal of Sound and Vibration, 458, 394-414.
7. Sapountzakis, E. J., & Mokos, V. G. (2007). Dynamic analysis of 3-D beam elements including warping and shear deformation effects. International Journal of Solids and Structures, 44(25-26), 8349-8370.
8. Fotouhi, R. (2007). Dynamic analysis of very flexible beams. Journal of Sound and Vibration, 305(3), 521-533.
9. Ghafari, E., & Rezaeepazhand, J. (2016). Vibration analysis of rotating composite beams using polynomial-based dimensional reduction method. International Journal of Mechanical Sciences, 115-116, 93-104.
10. Mehmood, A., Khan, A. A., & Rahman, H. (2014). Dynamic response analysis of functionally graded plates with moving mass using element-free Galerkin method. Mathematical Problems in Engineering, 2014, 1-15.
11. Sayyad, A. S., & Ghugal, Y. M. (2017). Modeling and analysis of functionally graded sandwich beams: A review. Mechanics of Advanced Materials and Structures, 24(8), 787-802.
12. Mazanoglu, K., Yesilyurt, I., & Sabuncu, M. (2009). Vibration analysis of multiple-cracked non-uniform beams. Journal of Sound and Vibration, 320(4-5), 977-989.
13. Avsec, J., & Oblak, M. (2007). Thermal vibrational analysis for simply supported beam and clamped beam. Journal of Sound and Vibration, 308(3-5), 514-525.
14. Wattanasakulpong, N., & Ungbhakorn, V. (2014). Linear and nonlinear vibration analysis of elastically restrained ends FGM beams with porosities. Aerospace Science and Technology, 32(1), 111-120.
15. Sharma, P., & Singh, R. (2021). A numerical study on free vibration analysis of axial FGM beam. Materials Today: Proceedings, 44, 1664-1668.
16. Xu, J., Yang, Z., Yang, J., & Li, Y. (2021). Free vibration analysis of rotating FG-CNT reinforced composite beams in thermal environments with general boundary conditions. Aerospace Science and Technology, 118, 107030.
17. Alebrahim, R., Haris, S. M., Mohamed, N. A. N., & Abdullah, S. (2015). Vibration analysis of self-healing hybrid composite beam under moving mass. Composite Structures, 119, 463-476.
18. Cheng, J., & Xiao, R. (2007). Probabilistic free vibration analysis of beams subjected to axial loads. Advances in Engineering Software, 38(1), 31-38.
19. Chalah-Rezgui, L., Chalah, F., Falek, K., Bali, A., & Nechnech, A. (2014). Transverse vibration analysis of uniform beams under various ends restraints. APCBEE procedia, 9, 328-333.
20. Liu, M.-F., & Chang, T.-P. (2005). Vibration analysis of a magneto-elastic beam with general boundary conditions subjected to axial load and external force. Journal of Sound and Vibration, 288(1-2), 399-411.
21. Vigneshwaran, K., & Behera, R. K. (2014). Vibration Analysis of a Simply Supported Beam with Multiple Breathing Cracks. Procedia Engineering, 86, 835-842.